Graduate School ETD Form 9
(Revised 01/14)

PURDUE UNIVERSITY
GRADUATE SCHOOL
Thesis/Dissertation Acceptance

This is to certify that the thesis/dissertation prepared

By Joonyong Lee

Entitled
THE FUNCTION OF ASCL1 IN PREGNANCY-INDUCED MATERNAL LIVER GROWTH

For the degree of Master of Science

Is approved by the final examining committee:

Guoli Dai

Teri Belecky-Adams

Jason S. Meyer

To the best of my knowledge and as understood by the student in the *Thesis/Dissertation Agreement. Publication Delay, and Certification/Disclaimer (Graduate School Form 32)*, this thesis/dissertation adheres to the provisions of Purdue University's "Policy on Integrity in Research" and the use of copyrighted material.

Guoli Dai

Approved by Major Professor(s): _____

_____

Approved by: Simon J. Atkinson 7/7/2014

Head of the Department Graduate Program Date

THE FUNCTION OF ASCL1 IN PREGNANCY-INDUCED MATERNAL LIVER GROWTH

A Thesis

Submitted to the Faculty

of

Purdue University

by

Joonyong Lee

In Partial Fulfillment of the

Requirements for the Degree

of

Master of Science

August 2014

Purdue University

Indianapolis, Indiana

ACKNOWLEDGMENTS

I would like to express my very great appreciation to Dr. Guoli Dai for his guidance and advice of this research work. I would also like to thank my committee members, Dr. Jason Meyer and Dr. Teri Belecky-Adams, for their support and invaluable suggestions.

I would also like to extend my thanks to my laboratory members: Dr. Yuhong Zou, Wenjuan Rui, Shashank M. Nambiar, Dr. Min Hu, and Sudhanshu Kumar.

Finally, I wish to thank my parents for their support and encouragement throughout my study.

TABLE OF CONTENTS

Page

LIST OF FIGURES

LIST OF ABBREVIATIONS

Ascl1	Achaete-Scute Complex Homolog 1
bHLH	Basic Helix-Loop-Helix
cDNA	Complementary DNA
CT	Comparative Cyclic Threshold
DAPI	4’,6-diamidino-2-phenylindole
EYFP	Enhanced Yellow Fluorescent Protein
FFPE	Formalin Fixed and Paraffin Embedded
KO	Knockout (Ascl1$^{flox/flox}$;R26$^{rtTA/rtTA}$;tetO-cre$^{tg/-}$) Mice
LPC	Liver Progenitor Cell
mRNA	Messenger Ribonucleic Acid
PCR	Polymerase Chain Reaction
PHx	Partial Hepatectomy
qRT-PCR	Quantitative Real-Time Polymerase Chain Reaction
R26	Rosa26 promoter element
RNA	Ribonucleic Acid
RT-PCR	Reverse Transcription Polymerase Chain Reaction
rtTA	Reverse Tetracycline-Controlled Transactivator
WT	Wild-type (Ascl1$^{wt/wt}$;R26$^{rtTA/rtTA}$;tetO-cre$^{tg/-}$) Mice

ABSTRACT

Lee, Joonyong M.S., Purdue University, August 2014. The function of *Ascl1* in pregnancy-induced maternal liver growth. Major Professor: Guoli Dai.

The maternal liver shows marked growth during pregnancy to accommodate the development and metabolic needs of the placenta and fetus. Previous study has shown that the maternal liver grows proportionally to the increase in body weight during gestation by hyperplasia and hypertrophy of hepatocytes. As the maternal liver is enlarged, the transcript level of *Ascl1*, a transcription factor essential to progenitor cells of the central nervous system and peripheral nervous system, is highly upregulated. The aims of the study were to (1) identify hepatic *Ascl1*-expressing cells, and (2) study the functions of *Ascl1* in maternal liver during pregnancy. *In situ* hybridization shows that most cell types (parenchymal, nonparenchymal, and mesothelial cells) express *Ascl1* mRNA in maternal livers during gestation and in male regenerating livers. Notably, hepatic mesothelial cells abundantly express *Ascl1* during pregnancy and liver regeneration. Inducible ablation of *Ascl1* gene during pregnancy results in maternal liver enlargement, litter size reduction, and fetal growth retardation. In addition, maternal hepatocytes deficient in *Ascl1* gene lack majority of their cytosols and exhibit β-catenin nuclear translocation, while maintaining their cellular boundary and identity. In summary, in both maternal liver during pregnancy and regenerating liver, the expression of *Ascl1* is

induced in most cell types. Mesothelial cells are potential origin of *Ascl1*-expressing cells. *Ascl1* gene is essential for the progression of normal pregnancy.

CHAPTER 1. INTRODUCTION

1.1 Objective

The objectives of the study were to identify hepatic *Ascl1*-expressing cells, and study the functions of *Ascl1* in maternal liver during pregnancy.

1.2 Background

1.2.1 Anatomy and function of the liver

Liver maintains homeostasis of the body via metabolism of carbohydrate, fat, and protein, storage of vitamins, processing of drugs and xenobiotics, and production of exocrine, bile acid, and bilirubin (Hill, 2009). Hepatocytes, the parenchymal cells of the liver, perform the majority of these vital functions and comprise about 80% of liver weight and 70% of total number of liver cells (Si-Tayeb et al., 2010). Fenestrated hepatic sinusoidal endothelial cells line hepatocytes and provide vascular supply from portal vein and hepatic artery, which flow into central vein. Hepatocytes secrete bile into bile canaliculi, which travels into bile ducts. The nonparenchymal cells of the liver are biliary epithelial cells, sinusoidal endothelial cells, Kupffer cells, pit cells, and hepatic stellate

cells. Biliary epithelial cells, or cholangiocytes, line bile ducts. Hepatic macrophages, also known as Kupffer cells, and hepatic natural killer cells, also called pit cells, play a role in liver defense mechanisms (Parker et al., 2012). Hepatic stellate cells, a population of hepatic fat storing cells, inhabit in the space of Disse, a perisinusoidal space between hepatocytes and sinusoidal endothelial cells (Friedman et al., 2008). Hence, the liver is comprised of heterogeneous populations of hepatic cells that maintain homeostatic balance.

1.2.2 Pregnancy-induced maternal liver growth

Various parts of maternal organs, such as pancreatic beta cells (Nielsen et al., 1999; Kim et al., 2010), forebrain subventricular zone (Shingo et al., 2003), and spleen (Bustamante et al., 2008), need to adapt to pregnancy for accommodating the development and metabolic needs of the placenta and fetus. The maternal liver shows marked growth during pregnancy (Bustamante et al., 2010). Proportional to the increase in body weight from the growth of fetus and placenta, the maternal liver grows 80% in size and doubles the weight by hyperplasia and hypertrophy of hepatocytes (Dai et al., 2011). The liver weight reverts to prepregnancy state after parturition. The maternal liver activates genes associated with liver growth and regeneration (cyclins A2, D1, and E, c-Jun, IL1β, IL6, and TNFα). Recent investigation shows that Nrf2, a transcription factor that regulates liver regeneration (Beyer et al., 2008; Wakabayashi et al., 2010), is required for normal maternal liver adaptation in response to pregnancy (Zou et al., 2013). Thus, maternal liver growth and liver regeneration may hold common themes.

1.2.3 Liver regeneration

The liver has a high capacity to regenerate from injuries. A model for acute liver injury is 2/3 partial hepatectomy (PHx). The mouse liver has five lobes (right and left medial lobes, right and left lateral lobes, and caudate lobe) and PHx is the surgical removal of right and left medial lobes and left lateral lobe (Mitchell and Willenbring, 2008). Hepatocytes have a slow turnover rate. In normal homeostatic environment, mature hepatocytes have a lifespan of 191 to 453 days (MacDonald, 1961) and divide twice in 300 days (Magami et al., 2002). However, hepatocytes undergo hypertrophy and hyperplasia to restore the normal liver-to-body weight ratio (~5%) after PHx (Miyaoka and Miyajima, 2013). Hepatocytes increase in cell size by 1.6-fold and 40% of hepatocytes undergo cell division to restore liver mass within 1 to 2 weeks after PHx. The current consensus is that only residual liver cells participate in liver regeneration after PHx and does not involve liver progenitor cells.

When the self-renewal capacity of hepatocytes is insufficient or blocked, liver progenitor cells (LPCs) take over to restore the liver. Chronic liver injuries, such as injuries induced by dipin (Factor et al., 1994), 3,5-diethoxycarbonyl-1,4-dihidro-collidine (DDC) (Preisegger et al., 1999), and high-fat diet with ethanol (Jung et al., 2008), activate proliferation and differentiation of LPCs. Small and oval shaped LPCs reside in the canal of Hering, the intermediate junction between hepatocytes and biliary epithelial cells (Paku et al., 2001). Cellular markers used for isolating LPCs are CD133, CD13, and Epcam in normal, acutely injured, and chronically injured adult livers (Rountree et al., 2007; Kamiya et al., 2009; Okabe et al., 2009). LPCs have high clonogenic properties,

the capability to differentiate into hepatocytes and biliary epithelial cells, and the ability to repopulate liver cells (Kamiya et al., 2009). However, bidirectional differentiations of LPCs into hepatocytes and biliary epithelial cells *in vivo* remain elusive.

1.2.4 Achaete-scute complex homolog 1

Cytogenetically located on chromosome 10, at 10 C1 in mouse, achaete-scute homolog 1 (*Ascl1* – Mouse Genome Informatics), formally known as mammalian achaete-scute homolog 1 (Mash1), is a member of the basic helix-loop-helix (bHLH) family of transcription factors that regulate neurogenesis and gliogenesis during development (Bertrand et al., 2002; Ross et al., 2003). The length of *Ascl1* gene is 2,620 base pairs, composed of two exons and one intron, while the protein is 231 amino acids long. Homo- or heterodimerization with other ubiquitously expressed bHLH proteins, such as E12 (Farah et al., 2000) and E47 (Massari and Murre, 2000), is necessary for efficient binding to an E box (CANNTG) of *Ascl1* target gene promoters. The target genes of *Ascl1* are transcription factors, such as NeuroD (Ma et al., 1996; Cau et al., 1997), Math4C and Ngn1 (Cau et al., 1997), Dlx1 and Dlx2 (Yun et al., 2002; Schuurmans et al., 2004; Poitras et al., 2007), Tlx3 and Ptf1a (Mizuguchi et al., 2006), and Olig2 and Nkx2-2 (Sugimori et al., 2008). In addition, *Ascl1* regulates proliferation and cell cycle exit genes, such as Cdk1, Cdc25b, Hipk2, and Prmt2 (Castro et al., 2011). *Ascl1* expression is essential to progenitor cells of the central nervous system (CNS) and peripheral nervous system (PNS). *Ascl1* is required for proper development and differentiation of olfactory sensory neurons (Guillemot et al., 1993; Cau et al., 1997),

pulmonary neuroendocrine cells (Borges et al., 1997; Ito et al., 2000), parafollicular cells (Lanigan et al., 1998), chromaffin cells (Huber et al., 2002), glomus cells (Kameda, 2005), and oligodendrocytes (Petryniak et al., 2007). Overexpression of *Ascl1* results in neuronal reprogramming from astrocytes (Berninger et al., 2007) and fibroblasts (Vierbuchen et al., 2010). Moreover, transfection of *Ascl1* is sufficient to differentiate embryonic carcinoma cells into neurons (Polyak et al., 1994; Farah et al., 2000). Thus, *Ascl1* gene is vital for the survival of the organism.

1.3 Hypothesis

Ascl1 plays a role in maternal hepatic adaptations to pregnancy.

CHAPTER 2. MATERIALS AND METHODS

2.1 Mouse Models

2.1.1 Animal care

Mice were allowed free access to food and water. The animals were maintained on 12 hour/12hour light/dark cycle at 22±1°C. All of the animal experiments were operated in accordance with the National Institutes of Health Guide for the Care and Use of Laboratory Animals. Protocols for the care and use of animals were accepted by the Indiana University-Purdue University Indianapolis Animal Care and Use Committee.

2.1.2 Ascl1$^{flox/flox}$;R26$^{rtTA/rtTA}$;tetO-cre$^{tg/-}$ mice

This mouse strain was generated to create an inducible *Ascl1* knockout mouse model by sequential breeding of following mouse strains.

B6.Cg-Gt(ROSA)26Sor$^{tm1(rtTA*M2)Jae}$/J mice (Stock #006965) were obtained from The Jackson Laboratory (Bar Harbor, ME). Genotyping was performed as per directions from the vendor. The following primers were used for genotyping R26 wild-type allele: forward 5'-AAAGTCGCTCTGAGTTGTTAT-3' and reverse 5'-GGAGCGGGAGAAA

TGGATATG-3’. Genotyping of R26 mutant allele was performed with the same forward primer as for the wild-type allele and the following reverse primer 5’-GCGAAGAGTTT GTCCTCAACC-3'. PCR conditions were 35 cycles of 94°C/30 sec; 65°C/1 min; 72°C/1 min. The expected results for wild-type band is around 650 bp while mutant band is 340 bp.

B6.Cg-Tg(tetO-cre1Jaw/J mice (Stock #006234) were obtained from The Jackson Laboratory (Bar Harbor, ME). Genotyping was performed as per directions from the vendor. The following primers were used for genotyping internal positive control: forward 5’-CTAGGCCACAGAATTGAAAGATCT-3’ and reverse 5’-GTAGGTGGAA ATTCTAGCATCATCC-3’. Genotyping of transgene was performed with the following primers: forward 5’-GCGGTCTGGCAGTAAAAACTATC-3’ and reverse 5’-GTGAAA CAGCATTGCTGTCACTT-3’. PCR conditions were 35 cycles of 94°C/30 sec; 70°C/1 min; 72°C/1 min. The expected results for internal positive control band is 324 bp while transgene band is around 100 bp. This assay does not distinguish between hemizygote from homozygote transgenic mice.

Ascl1$^{flox/flox}$;R26$^{stopfloxYFP/stofloxYFP}$ mice were generous gifts from Dr. Guillemot (MRC National Institute for Medical Research, Mill Hill, London). Genotyping was performed as per directions (Pacary et al., 2011) with modifications. The following primers were used for genotyping *Ascl1* wild-type allele: forward 5’-CTACTGTCCAAA CGCAAAGTGG-3’ and reverse 5’-GCTCCCACAATCCTCGTAAAGA-3’. Genotyping of *Ascl1* mutant allele was performed with the same forward primer as for the wild-type allele and the following reverse primer 5’-TAGACGTTGTGGCTGTTGTAGT-3'. PCR conditions were 35 cycles of 94°C/30 sec; 69°C/30 sec; 72°C/90 sec. The expected

results for wild-type band is 342 bp while mutant band is 857 bp. The following primers were used for genotyping R26 wild-type allele: forward 5'-AAAGTCGCTCTGAGTTGTTAT-3' and reverse 5'-GGAGCGGGAGAAATGGATATG-3'. Genotyping of R26 mutant allele was performed with the same forward primer as for the wild-type allele and the following reverse primer 5'-AAGACCGCGAAGAGTTTGTC-3'. PCR conditions were 35 cycles of 94°C/30 sec; 69°C/1 min; 72°C/1 min. The expected results for wild-type band is 600 bp while mutant band is 320 bp.

R26$^{rtTA/rtTA}$ mice were crossed with tetO-cre$^{tg/-}$ mice to produce R26$^{rtTA/rtTA}$;tetO-cre$^{tg/-}$ mice. The progenies were then bred with Ascl1$^{flox/flox}$;R26$^{stopfloxYFP/stofloxYFP}$ mice. Since both Enhanced Yellow Fluorescent Protein (EYFP) and reverse tetracycline-controlled transactivator (rtTA) genes occupied the same R26 promoter element, the EYFP gene was removed by artificial selection. Extensive selective breeding was performed to generate *Ascl1* inducible knockout mice (Ascl1$^{flox/flox}$;R26$^{rtTA/rtTA}$;tetO-cre$^{tg/-}$) and wild-type control mice (Ascl1$^{wt/wt}$;R26$^{rtTA/rtTA}$;tetO-cre$^{tg/-}$).

2.1.3 Ascl1$^{flox/CreERT2}$;R26$^{stopfloxYFP/stopfloxYFP}$ mice

This mouse strain was generated to create a conditional and inducible *Ascl1* knockout mouse model by sequential breeding of Ascl1$^{tm1.1(Cre/ERT2)Jejo}$/J mice (Stock #012882) obtained from The Jackson Laboratory (Bar Harbor, ME). Genotyping was performed as per directions from the vendor. The following primers were used for genotyping *Ascl1* wild-type allele: forward 5'-TCCAACGACTTGAACTCTATGG-3' and reverse 5'-CCAGGACTCAATACGCAGGG-3'. Genotyping of *Ascl1* mutant allele

was performed with the following primers: forward 5'-AACTTTCCTCCGGGGCTCGT TTC-3' and reverse primer 5'-CGCCTGGCGATCCCTGAACATG-3'. Hotstart Taq polymerase was used for the assay. PCR conditions were 35 cycles of 94°C/30 sec; 62°C/30 sec; 72°C/30 sec. The expected results for wild-type band is 418bp while mutant band is around 300 bp. Ascl1$^{flox/flox}$;R26$^{stopfloxYFP/stofloxYFP}$ mice are described above in the same page. Ascl1$^{Cre/+}$ mice were crossed with Ascl1$^{flox/flox}$;R26$^{stopfloxYFP/stofloxYFP}$ mice. Selective breeding was performed to generate *Ascl1* conditional and inducible knockout mice (Ascl1$^{flox/CreERT2}$;R26$^{stopfloxYFP/stopfloxYFP}$) and wild-type control mice (Ascl1$^{flox/wt}$;R26$^{stopfloxYFP/stopfloxYFP}$).

2.2 Timed pregnancy

Ascl1 inducible knockout and wild-type control female mice were bred with wild-type control male mice to ensure that fetuses have at least one *Ascl1* gene after doxycycline treatment. Breeding cages were setup and the presence of a copulation plug in the vagina was considered as gestation day 1. Plug-positive female mice were housed separately from male mice.

2.3 Tissue collection

Pregnant mice were administered with doxycycline (1 mg/ml) in drinking water from gestation day 6 to 18. Mice were sacrificed by cervical dislocation and weighed. Livers were dissected and weighed. Liver tissues were fixed in formalin and sent to

Indiana University pathology core to be embedded in paraffin for histological analysis or snap-frozen in liquid nitrogen for total RNA isolation.

2.4 Quantitative real-time polymerase chain reaction

Total RNA was isolated from frozen liver tissue using TRIzol reagent according to the manufacturer's protocol (Invitrogen, Carlsbad, CA). cDNA was synthesized from each sample using Verso cDNA kit (Thermo Scientific, Rockford, IL), diluted 4 times with water, and subjected to qRT-PCR to quantify mRNA levels. TaqMan Universal PCR Master Mix and *Ascl1* TaqMan probe (Mm04207567_g1) were used from Applied Biosystems (Foster City, CA). The amplification reactions were carried out in the ABI Prism 7900 sequence detection system (Applied Biosystems, Foster City, CA) with initial hold steps (50°C for 2 minutes followed by 95°C for 10 minutes) and 40 cycles of a two-step PCR (92°C for 15 seconds and 60°C for 1 minute). The comparative CT method was used for relative quantification of the amount of mRNA for each sample normalized to Albumin transcript levels.

2.5 Hepatocyte density measurement

Formalin-fixed and paraffin-embedded liver sections were stained with Hematoxylin and Eosin. Hepatocytes were counted with Image-Pro Plus software (Media Cybernetics, MD) in five microscope fields at 400x magnification. This technique was consistent for each sample.

2.6 Immunohistochemistry

Formalin-fixed and paraffin-embedded liver sections were subjected to pan cadherin and HNF4α immunostaining for visualizing hepatic cell boundary and evaluating hepatocyte identity, respectively. Livers sectioned at 5 μm were deparaffinized and hydrated. Epitope retrieval was performed by placing the slides into boiling citrate buffer (10 mM, pH 6.0) for 30 minutes and cooled to room temperature for 3 hours. Endogenous peroxidase activity was quenched using 3% H_2O_2 for 10 minutes. Sections were blocked with normal serum of the animal that the secondary antibody was raised for 1 hour at room temperature. Afterwards, sections were incubated with a primary antibody against pan cadherin (Cell Signaling, Cat #4068; 1:100) or HNF4α (Santa Cruz, Cat #sc-6556; 1:50) at 4°C overnight. On the following day, sections were incubated with respective biotinylated secondary antibody for 1 hour at room temperature, VECTASTAIN ABC Kit reagent for 30 minutes (Vector Laboratories, Burlingame, CA), and DAB Peroxidase Substrate Kit reagent (Vector Laboratories, Burlingame, CA) according to the manufacturer's instructions. Sections were counterstained with hematoxylin, dehydrated, and mounted with coverslip.

2.7 Immunofluorescence

Formalin-fixed and paraffin-embedded liver sections were subjected to β-catenin immunofluorescence staining for visualizing nuclear localization in hepatic cells. Livers sectioned at 5 μm were deparaffinized, epitopes retrieved, endogenous peroxidase

quenched, and blocked as described above. Sections were incubated with a primary antibody against β-catenin (BD Transduction, Cat #610153; 1:20) at 4°C overnight. On the following day, sections were incubated with fluorescent-tagged secondary antibody (Jackson ImmunoResearch Laboratories, West Grove, PA) for 1 hour at room temperature in the dark. The slides were mounted using ProLong Gold Antifade Mountant with DAPI (Life Technologies, Carlsbad, CA) and examined under confocal microscopy (Olympus FluoView FV1000).

2.8 *Ascl1* mRNA *in situ* hybridization

Livers of partially hepatectomized C57BL6 male mice and gestation day 11 CD1 female mice were fixed in formalin, embedded in paraffin, and sectioned at 5 μm from Indiana University pathology core. *In situ* hybridization procedures for mouse *Ascl1* mRNA and Fast Red staining on the hybridized probes were performed by the RNAscope 2.0 Formalin-Fixed, Paraffin-Embedded (FFPE) Assay (Advanced Cell Diagnostics, Inc., Hayward, CA) and a probe for mouse *Ascl1* mRNA (NM_008553, Advanced Cell Diagnostics) according to the manufacturer's instruction. Trial experiments using negative control DapB (dihydrodipicolinate reductase) and positive control Ppib (peptidylprolyl isomerase B) mRNAs were tested to determine the efficiency of the standardized protocol.

CHAPTER 3. RESULTS

3.1 Identification of cells expressing *Ascl1* mRNA in maternal liver during pregnancy

To determine *Ascl1*-expressing cells in maternal liver, *in situ* hybridization was performed using *Ascl1* mRNA probe on liver sections from nonpregnant, gestation day 11, and gestation day 18 CD1 mice. Nonpregnant livers were negative for *Ascl1* mRNA. In contrast, *Ascl1* mRNA expression was widely distributed in pregnant livers, including parenchymal, nonparenchymal, and mesothelial cells (**Figure 1**). Within *Ascl1*-positive hepatic parenchymal cells, *Ascl1* mRNA was predominantly located in the nucleus. The data demonstrate that *Ascl1* mRNA is expressed in most cell types in maternal liver during gestation.

3.2 Identification of cells expressing *Ascl1* mRNA in regenerating liver

To determine *Ascl1*-expressing cells in regenerating adult liver, *in situ* hybridization was performed using *Ascl1* mRNA probe on liver sections from 2/3 partially hepatectomized (PHx) C57BL/6J male mice. In normal liver, small populations of *Ascl1*-expressing cells were observed on outer edge and in periportal region. In regenerating liver, however, *Ascl1*-expressing cells were widely distributed in multiple

hepatic cell types (**Figure 2**). Until 24 hours after PHx, *Ascl1*-expressing cells only consisted small populations of liver cells. From 36 to 140 hours after PHx, most hepatic parenchymal, nonparenchymal, and mesothelial cells were expressing *Ascl1* mRNA. By the end of liver regeneration (168 hours after PHx), *Ascl1*-expressing cells were mostly observed on outer edge and in periportal region. In addition, *Ascl1* mRNA was primarily localized in the nuclei of hepatic cells. Thus, hepatic *Ascl1* transcription is activated after PHx and most hepatic cell types express *Ascl1* mRNA during liver regeneration.

3.3 Study of global loss-of-function of *Ascl1*

3.3.1 Generation of global inducible *Ascl1* knockout mouse model

A mouse strain (Ascl1$^{flox/flox}$;R26$^{rtTA/rtTA}$;tetO-cre$^{tg/-}$) was generated to study the function of *Ascl1* (see **Materials and Methods**). This mouse strain carries loxP-flanked *Ascl1* gene, reverse tetracycline-controlled transactivator (rtTA) gene under control of ubiquitous Rosa26 promoter element, and Cre recombinase gene under control of tetracycline-responsive promoter element. Administration of doxycycline activates rtTA, which drives Cre recombinase expression to delete *Ascl1* gene (**Figure 3**). However, the cells in the brain and testis are not affected since doxycycline is unable to travel across the blood-brain and blood-testis barriers (Hochedlinger et al., 2005). A control mouse strain (Ascl1$^{wt/wt}$;R26$^{rtTA/rtTA}$;tetO-cre$^{tg/-}$) was also generated as a genetic control. In this mouse strain, *Ascl1* gene lacks loxP sites, and thus, doxycycline treatment does not ablate *Ascl1* gene.

3.3.2 Phenotype analysis of global inducible *Ascl1* knockout

3.3.2.1 Global inducible *Ascl1* knockout causes maternal liver enlargement, litter size reduction, and fetal growth retardation

To identify the phenotype from *Ascl1* ablation, genetic control (WT) and *Ascl1* inducible knockout (KO) pregnant mice were treated with doxycycline in drinking water (1 mg/ml) from gestation day 6 (D6) until gestation day 18 (D18). On D18, the maternal livers and fetuses were collected and weighed. KO maternal livers had successfully deleted *Ascl1* gene based on quantitative real-time polymerase chain reaction (qRT-PCR) (**Figure 4**). KO maternal livers showed 99% decrease in *Ascl1* mRNA expression when compared to controls. Deletion of *Ascl1* gene during gestation resulted in increased liver-to-body weight ratio (5.4% in WT vs. 6.9% in KO), 35% decrease in litter size, and 18% decrease in fetal weight when compared to controls (**Figure 5**). These results indicated that *Ascl1* is essential for normal pregnancy.

3.3.2.2 Global ablation of *Ascl1* causes abnormalities in maternal liver histology and nuclear translocation of β-catenin in maternal liver cells during gestation

Due to abnormal size of maternal livers in *Ascl1* KO mice, histological analysis was performed to gain insight into the phenotype. Hematoxylin and eosin (H&E) staining showed normal histological sections in WT livers while deficiency of cytosol around nuclei of hepatocytes in KO livers were observed (**Figure 6**). Morphologically, cell

boundaries were not readily apparent in KO livers in comparison to WT livers. However, pan cadherin staining result suggested normal cell-cell adhesion in liver parenchyma (**Figure 7**). In addition, hepatocytes showed positive hepatocyte nuclear factor 4 alpha (HNF4α) nuclear staining regardless of genotype (**Figure 8**). This observation suggested hepatocyte identity was not impaired with *Ascl1* ablation. Interestingly, β-catenin was weakly detected in the nucleus of WT liver cells (**Figure 9**). In contrast, the nuclear β-catenin was abundant in the nucleus of KO liver cells. Therefore, ablation of *Ascl1* gene resulted in nuclear translocation of β-catenin. Taken together, *Ascl1* ablation resulted in changes at molecular, cellular, and organ levels in the maternal livers.

3.4 Study of cell-specific loss-of-function of *Ascl1*

3.4.1 Generation of cell-specific conditional and inducible *Ascl1* knockout mouse model

A mouse strain ($Ascl1^{flox/CreERT2}$;$R26^{stopfloxYFP/stopfloxYFP}$) was generated to study the function of *Ascl1* (see **Materials and Methods**). This mouse strain carries loxP-flanked *Ascl1* gene, loxP-flanked STOP sequence followed by Enhanced Yellow Fluorescent Protein gene (EYFP) under control of Rosa26 promoter element, and Cre recombinase gene under control of *Ascl1* promoter element. *Ascl1*-expressing cells produce Cre recombinase, which ablates *Ascl1* gene and STOP sequence with the administration of tamoxifen (**Figure 10**). As a result, *Ascl1*-expressing cells ablates *Ascl1* while permanently being labeled with EYFP. A control mouse strain ($Ascl1^{CreERT2/wt}$;$R26^{stopfloxYFP/stopfloxYFP}$) was also generated. In this mouse strain, *Ascl1*

gene lacks loxP sites, and thus, tamoxifen treatment does not ablate *Ascl1*. This control mouse strain can be used to label *Ascl1*-expressing cells with EYFP and study the faith of these cells when tamoxifen is administered. In KO mouse strain, *Ascl1*-expressing cells are labeled with EYFP and *Ascl1* gene is deleted with administration of tamoxifen. Thus, in this mouse strain, the effect of *Ascl1* ablation in *Ascl1*-expressing cells can be evaluated. The mouse strains have been primarily evaluated for phenotypes. Preliminary study indicates enlargement of maternal liver as seen with doxycycline mouse model. Currently, the expansion of the two colonies is in process.

CHAPTER 4. DISCUSSION

We demonstrate for the first time that pregnant and regenerating liver activates *Ascl1* transcription. In maternal livers, previous RT-PCR analysis showed that expression of *Ascl1* mRNA begins from gestation day 8 to the end of pregnancy (unpublished data). Here, we demonstrate by *in situ* hybridization that multiple cell types (parenchymal, nonparenchymal, and mesothelial cells) in maternal liver express *Ascl1*. During liver regeneration, multiple hepatic cell types express *Ascl1* from 36 to 168 hours after PHx. During development, progenitor cells in central nervous system (CNS) and peripheral nervous system (PNS) express *Ascl1*, including neuroblasts (Tomita et al., 2000), telencephalic progenitor cells (Casarosa et al., 1999; Parras et al., 2002; Yun et al., 2002), oligodendrocyte precursor cells (Petryniak et al., 2007), late dorsal precursor cells (Mizuguchi et al., 2006), olfactory receptor neuron progenitor cells (Cau et al., 1997; Murray et al., 2003; Krolewski et al., 2012), retinal progenitor cells (Tomita et al., 1996, 2000; Hatakeyama et al., 2001; Nelson et al., 2009), pulmonary neuroendocrine progenitor cells (Borges et al., 1997), and gastric neuroendocrine progenitor cells (Kokubu et al., 2008). In adult mice, pituitary and microglia express *Ascl1* (www.BioGPS.org). Moreover, neuroendocrine tumors, such as small cell lung cancers (Ball, 2004), medullary thyroid cancers (Chen et al., 2005), gastroenteropancreatic neuroendocrine tumors (Shida et al., 2008), and prostate cancers (Vias et al., 2008), also

express *Ascl1*. Our findings link *Ascl1* gene with liver growth in both physiological and pathological conditions in adult animals.

Notably, hepatic mesothelial cells abundantly express *Ascl1* during pregnancy and liver regeneration. During liver fibrogenesis, hepatic mesothelial cells expressing Wilms tumor 1 undergo mesothelial-mesenchymal transition to generate hepatic stellate cells and myofibroblasts (Li et al., 2013), indicating mesothelial cells as one type of liver progenitor cells. In addition, a small area of mesothelium in mouse ovary contains a stem cell niche of the ovarian surface epithelium (Flesken-Nikitin et al., 2013). Based on these two reports, we strongly believe that hepatic mesothelial cells are potentially liver progenitor cells expressing *Ascl1* during pregnancy and liver regeneration. Further studies are needed to determine this.

We also demonstrate that the mouse model efficiently ablates *Ascl1* gene during gestation, and results in maternal liver enlargement, litter size reduction, and fetal growth retardation. In addition, maternal hepatocytes deficient in *Ascl1* gene lack majority of their cytosols while maintaining their cellular boundary and identity. The functions of *Ascl1* in nervous system have been intensively investigated. *Ascl1* regulates proliferation, cell cycle exit, and differentiation during neurogenesis. *Ascl1* promotes progenitor divisions by positively regulating G1/S transition and entry into mitosis (Castro et al., 2006, 2011). Moreover, *Ascl1* terminates proliferation of progenitors by targeting cell cycle arrest genes, such as Ccng2, Fbxw7, and Gadd45g, during late phase of neurogenesis (Farah et al., 2000; Nakada et al., 2004; Castro et al., 2011). Finally, *Ascl1* acts on differentiation and maturation of progenitor cells by regulating downstream neural transcription factors, including Dlx2, Ebf3, and Gli3 (Anderson et al., 1997;

Kuschel et al., 2003; Steele-Perkins et al., 2005; Bergsland et al., 2006; Zhao et al., 2006; Petryniak et al., 2007). Hence, *Ascl1* has roles in all stages of neurogenesis. The phenotype of *Ascl1* gene deletion during gestation indicate its essential roles in maintaining normal pregnancy. The functions of *Ascl1* during pregnancy and liver regeneration require further investigations. The animal models that we have generated have proven to be a useful *in vivo* approach to pursue this goal.

Prior to parturition, maternal livers of *Ascl1* knockout mice showed accumulation of β-catenin in the nuclei of hepatocytes. β-catenin, a transcription factor, is a critical component in embryonic development and stem cell maintenance. Normally restricted in cell adhesion complex, β-catenin undergo phosphorylation by casein kinase 1 (CK1) and glycogen synthase kinase 3 (GSK3), ubiquitination, and degradation by proteasomes (Moon et al., 2004). When Wnt signaling pathway is active, β-catenin degradation decreases, accumulates in cytosol, translocates into cell nucleus, and interacts with T-cell factor (TCF) and lymphoid enhancer-binding protein (LEF) transcription factors to initiate activation of β-catenin target genes, such as neurogenin 1 (Hirabayashi et al., 2004), NeuroD1 (Kuwabara et al., 2009), cyclin D1, and EGF receptor (Tan et al., 2005). β-catenin also regulates liver homeostasis and regeneration (Monga et al., 2001). Both β-catenin knockdown and knockout suppress hepatocyte proliferation and delay liver regeneration after PHx (Sodhi et al., 2005; Tan et al., 2006). In addition, Wnt/β-catenin pathway regulates differentiation of liver progenitor cells into hepatocytes (Boulter et al., 2012). β-catenin nuclear translocation in *Ascl1* knockout liver strongly suggests that *Ascl1* genetic deletion results in the activation of Wnt/β-catenin pathway in hepatocytes.

This provides an important clue to understand how *Ascl1* exerts its regulatory effects in pregnant liver and, potentially, regenerating liver.

In summary, both maternal liver during pregnancy and regenerating liver after PHx induce expression of *Ascl1* in most hepatic cell types. *Ascl1* gene is essential for the progression of normal pregnancy. Mesothelial cells are potential origin of *Ascl1*-expressing cells. Future direction includes further identification of hepatic *Ascl1*-expressing cells, isolation and characterization of hepatic *Ascl1*-expressing cells, and further *Ascl1* functional studies.

REFERENCES

REFERENCES

1) Anderson, S. A., Qiu, M., Bulfone, A., Eisenstat, D. D., Meneses, J., Pedersen, R., & Rubenstein, J. L. (1997). Mutations of the homeobox genes Dlx-1 and Dlx-2 disrupt the striatal subventricular zone and differentiation of late born striatal neurons. *Neuron, 19*(1), 27-37.

2) Ball, D. W. (2004). Achaete-scute homolog-1 and Notch in lung neuroendocrine development and cancer. *Cancer Lett, 204*(2), 159-169. doi: 10.1016/s0304-3835(03)00452-x

3) Bergsland, M., Werme, M., Malewicz, M., Perlmann, T., & Muhr, J. (2006). The establishment of neuronal properties is controlled by Sox4 and Sox11. *Genes Dev, 20*(24), 3475-3486. doi: 10.1101/gad.403406

4) Berninger, B., Guillemot, F., & Gotz, M. (2007). Directing neurotransmitter identity of neurones derived from expanded adult neural stem cells. *Eur J Neurosci, 25*(9), 2581-2590. doi: 10.1111/j.1460-9568.2007.05509.x

5) Bertrand, N., Castro, D. S., & Guillemot, F. (2002). Proneural genes and the specification of neural cell types. *Nat Rev Neurosci, 3*(7), 517-530. doi: 10.1038/nrn874

6) Beyer, T. A., Xu, W., Teupser, D., auf dem Keller, U., Bugnon, P., Hildt, E., . . . Werner, S. (2008). Impaired liver regeneration in Nrf2 knockout mice: role of ROS-mediated insulin/IGF-1 resistance. *EMBO J, 27*(1), 212-223. doi: 10.1038/sj.emboj.7601950

7) Borges, M., Linnoila, R. I., van de Velde, H. J., Chen, H., Nelkin, B. D., Mabry, M., . . . Ball, D. W. (1997). An achaete-scute homologue essential for neuroendocrine differentiation in the lung. *Nature, 386*(6627), 852-855. doi: 10.1038/386852a0

8) Boulter, L., Govaere, O., Bird, T. G., Radulescu, S., Ramachandran, P., Pellicoro, A., . . . Forbes, S. J. (2012). Macrophage-derived Wnt opposes Notch signaling to specify hepatic progenitor cell fate in chronic liver disease. *Nat Med, 18*(4), 572-579. doi: 10.1038/nm.2667

9) Bustamante, J. J., Copple, B. L., Soares, M. J., & Dai, G. (2010). Gene profiling of maternal hepatic adaptations to pregnancy. *Liver Int, 30*(3), 406-415. doi: 10.1111/j.1478-3231.2009.02183.x

10) Bustamante, J. J., Dai, G., & Soares, M. J. (2008). Pregnancy and lactation modulate maternal splenic growth and development of the erythroid lineage in the rat and mouse. *Reprod Fertil Dev, 20*(2), 303-310.

11) Casarosa, S., Fode, C., & Guillemot, F. (1999). Mash1 regulates neurogenesis in the ventral telencephalon. *Development, 126*(3), 525-534.

12) Castro, D. S., Martynoga, B., Parras, C., Ramesh, V., Pacary, E., Johnston, C., . . . Guillemot, F. (2011). A novel function of the proneural factor Ascl1 in progenitor proliferation identified by genome-wide characterization of its targets. *Genes Dev, 25*(9), 930-945. doi: 10.1101/gad.627811

13) Castro, D. S., Skowronska-Krawczyk, D., Armant, O., Donaldson, I. J., Parras, C., Hunt, C., . . . Guillemot, F. (2006). Proneural bHLH and Brn proteins coregulate a neurogenic program through cooperative binding to a conserved DNA motif. *Dev Cell, 11*(6), 831-844. doi: 10.1016/j.devcel.2006.10.006

14) Cau, E., Gradwohl, G., Fode, C., & Guillemot, F. (1997). Mash1 activates a cascade of bHLH regulators in olfactory neuron progenitors. *Development, 124*(8), 1611-1621.

15) Chen, H., Kunnimalaiyaan, M., & Van Gompel, J. J. (2005). Medullary thyroid cancer: the functions of raf-1 and human achaete-scute homologue-1. *Thyroid, 15*(6), 511-521. doi: 10.1089/thy.2005.15.511

16) Dai, G., Bustamante, J. J., Zou, Y., Myronovych, A., Bao, Q., Kumar, S., & Soares, M. J. (2011). Maternal hepatic growth response to pregnancy in the mouse. *Exp Biol Med (Maywood), 236*(11), 1322-1332. doi: 10.1258/ebm.2011.011076

17) Factor, V. M., Radaeva, S. A., & Thorgeirsson, S. S. (1994). Origin and fate of oval cells in dipin-induced hepatocarcinogenesis in the mouse. *Am J Pathol, 145*(2), 409-422.

18) Farah, M. H., Olson, J. M., Sucic, H. B., Hume, R. I., Tapscott, S. J., & Turner, D. L. (2000). Generation of neurons by transient expression of neural bHLH proteins in mammalian cells. *Development, 127*(4), 693-702.

19) Flesken-Nikitin, A., Hwang, C. I., Cheng, C. Y., Michurina, T. V., Enikolopov, G., & Nikitin, A. Y. (2013). Ovarian surface epithelium at the junction area contains a cancer-prone stem cell niche. *Nature, 495*(7440), 241-245. doi: 10.1038/nature11979

20) Friedman, S. L. (2008). Hepatic stellate cells: protean, multifunctional, and enigmatic cells of the liver. *Physiol Rev, 88*(1), 125-172. doi: 10.1152/physrev.00013.2007

21) Guillemot, F., Lo, L. C., Johnson, J. E., Auerbach, A., Anderson, D. J., & Joyner, A. L. (1993). Mammalian achaete-scute homolog 1 is required for the early development of olfactory and autonomic neurons. *Cell, 75*(3), 463-476.

22) Hatakeyama, J., Tomita, K., Inoue, T., & Kageyama, R. (2001). Roles of homeobox and bHLH genes in specification of a retinal cell type. *Development, 128*(8), 1313-1322.

23) Hill, C. (2009). Anatomy and Physiology *Liver Diseases* (pp. 1-14): Wiley-Blackwell.

24) Hirabayashi, Y., Itoh, Y., Tabata, H., Nakajima, K., Akiyama, T., Masuyama, N., & Gotoh, Y. (2004). The Wnt/beta-catenin pathway directs neuronal differentiation of cortical neural precursor cells. *Development, 131*(12), 2791-2801. doi: 10.1242/dev.01165

25) Hochedlinger, K., Yamada, Y., Beard, C., & Jaenisch, R. (2005). Ectopic expression of Oct-4 blocks progenitor-cell differentiation and causes dysplasia in epithelial tissues. *Cell, 121*(3), 465-477. doi: 10.1016/j.cell.2005.02.018

26) Huber, K., Bruhl, B., Guillemot, F., Olson, E. N., Ernsberger, U., & Unsicker, K. (2002). Development of chromaffin cells depends on MASH1 function. *Development, 129*(20), 4729-4738.

27) Ito, T., Udaka, N., Yazawa, T., Okudela, K., Hayashi, H., Sudo, T., . . . Kitamura, H. (2000). Basic helix-loop-helix transcription factors regulate the neuroendocrine differentiation of fetal mouse pulmonary epithelium. *Development, 127*(18), 3913-3921.

28) Jung, Y., Brown, K. D., Witek, R. P., Omenetti, A., Yang, L., Vandongen, M., . . . Diehl, A. M. (2008). Accumulation of hedgehog-responsive progenitors parallels alcoholic liver disease severity in mice and humans. *Gastroenterology, 134*(5), 1532-1543. doi: 10.1053/j.gastro.2008.02.022

29) Kameda, Y. (2005). Mash1 is required for glomus cell formation in the mouse carotid body. *Dev Biol, 283*(1), 128-139. doi: 10.1016/j.ydbio.2005.04.004

30) Kamiya, A., Kakinuma, S., Yamazaki, Y., & Nakauchi, H. (2009). Enrichment and clonal culture of progenitor cells during mouse postnatal liver development in mice. *Gastroenterology, 137*(3), 1114-1126, 1126 e1111-1114. doi: 10.1053/j.gastro.2009.06.001

31) Kim, H., Toyofuku, Y., Lynn, F. C., Chak, E., Uchida, T., Mizukami, H., . . . German, M. S. (2010). Serotonin regulates pancreatic beta cell mass during pregnancy. *Nat Med, 16*(7), 804-808. doi: 10.1038/nm.2173

32) Kokubu, H., Ohtsuka, T., & Kageyama, R. (2008). Mash1 is required for neuroendocrine cell development in the glandular stomach. *Genes Cells, 13*(1), 41-51. doi: 10.1111/j.1365-2443.2007.01146.x

33) Krolewski, R. C., Packard, A., Jang, W., Wildner, H., & Schwob, J. E. (2012). Ascl1 (Mash1) knockout perturbs differentiation of nonneuronal cells in olfactory epithelium. *PLoS One, 7*(12), e51737. doi: 10.1371/journal.pone.0051737

34) Kuschel, S., Ruther, U., & Theil, T. (2003). A disrupted balance between Bmp/Wnt and Fgf signaling underlies the ventralization of the Gli3 mutant telencephalon. *Dev Biol, 260*(2), 484-495.

35) Kuwabara, T., Hsieh, J., Muotri, A., Yeo, G., Warashina, M., Lie, D. C., . . . Gage, F. H. (2009). Wnt-mediated activation of NeuroD1 and retro-elements during adult neurogenesis. *Nat Neurosci, 12*(9), 1097-1105. doi: 10.1038/nn.2360

36) Lanigan, T. M., DeRaad, S. K., & Russo, A. F. (1998). Requirement of the MASH-1 transcription factor for neuroendocrine differentiation of thyroid C cells. *J Neurobiol, 34*(2), 126-134.

37) Li, Y., Wang, J., & Asahina, K. (2013). Mesothelial cells give rise to hepatic stellate cells and myofibroblasts via mesothelial-mesenchymal transition in liver injury. *Proc Natl Acad Sci U S A, 110*(6), 2324-2329. doi: 10.1073/pnas.1214136110

38) Ma, Q., Kintner, C., & Anderson, D. J. (1996). Identification of neurogenin, a vertebrate neuronal determination gene. *Cell, 87*(1), 43-52.

39) Macdonald, R. A. (1961). "Lifespan" of liver cells. Autoradio-graphic study using tritiated thymidine in normal, cirrhotic, and partially hepatectomized rats. *Arch Intern Med, 107*, 335-343.

40) Magami, Y., Azuma, T., Inokuchi, H., Kokuno, S., Moriyasu, F., Kawai, K., & Hattori, T. (2002). Cell proliferation and renewal of normal hepatocytes and bile duct cells in adult mouse liver. *Liver, 22*(5), 419-425.

41) Massari, M. E., & Murre, C. (2000). Helix-loop-helix proteins: regulators of transcription in eucaryotic organisms. *Mol Cell Biol, 20*(2), 429-440.

42) Mitchell, C., & Willenbring, H. (2008). A reproducible and well-tolerated method for 2/3 partial hepatectomy in mice. *Nat Protoc, 3*(7), 1167-1170. doi: 10.1038/nprot.2008.80

43) Miyaoka, Y., & Miyajima, A. (2013). To divide or not to divide: revisiting liver regeneration. *Cell Division, 8*(1), 8.

44) Mizuguchi, R., Kriks, S., Cordes, R., Gossler, A., Ma, Q., & Goulding, M. (2006). Ascl1 and Gsh1/2 control inhibitory and excitatory cell fate in spinal sensory interneurons. *Nat Neurosci, 9*(6), 770-778. doi: 10.1038/nn1706

45) Monga, S. P., Pediaditakis, P., Mule, K., Stolz, D. B., & Michalopoulos, G. K. (2001). Changes in WNT/beta-catenin pathway during regulated growth in rat liver regeneration. *Hepatology, 33*(5), 1098-1109. doi: 10.1053/jhep.2001.23786

46) Moon, R. T., Kohn, A. D., Ferrari, G. V. D., & Kaykas, A. (2004). WNT and [beta]-catenin signalling: diseases and therapies. *Nat Rev Genet, 5*(9), 691-701.

47) Murray, R. C., Navi, D., Fesenko, J., Lander, A. D., & Calof, A. L. (2003). Widespread defects in the primary olfactory pathway caused by loss of Mash1 function. *J Neurosci, 23*(5), 1769-1780.

48) Nakada, Y., Hunsaker, T. L., Henke, R. M., & Johnson, J. E. (2004). Distinct domains within Mash1 and Math1 are required for function in neuronal differentiation versus neuronal cell-type specification. *Development, 131*(6), 1319-1330. doi: 10.1242/dev.01008

49) Nelson, B. R., Hartman, B. H., Ray, C. A., Hayashi, T., Bermingham-McDonogh, O., & Reh, T. A. (2009). Acheate-scute like 1 (Ascl1) is required for normal delta-like (Dll) gene expression and notch signaling during retinal development. *Dev Dyn, 238*(9), 2163-2178. doi: 10.1002/dvdy.21848

50) Nielsen, J. H., Svensson, C., Galsgaard, E. D., Moldrup, A., & Billestrup, N. (1999). Beta cell proliferation and growth factors. *J Mol Med (Berl), 77*(1), 62-66.

51) Okabe, M., Tsukahara, Y., Tanaka, M., Suzuki, K., Saito, S., Kamiya, Y., . . . Miyajima, A. (2009). Potential hepatic stem cells reside in EpCAM+ cells of normal and injured mouse liver. *Development, 136*(11), 1951-1960. doi: 10.1242/dev.031369

52) Paku, S., Schnur, J., Nagy, P., & Thorgeirsson, S. S. (2001). Origin and structural evolution of the early proliferating oval cells in rat liver. *Am J Pathol, 158*(4), 1313-1323. doi: 10.1016/s0002-9440(10)64082-5

53) Parker, G. A., & Picut, C. A. (2012). Immune functioning in non lymphoid organs: the liver. *Toxicol Pathol, 40*(2), 237-247. doi: 10.1177/0192623311428475

54) Parras, C. M., Schuurmans, C., Scardigli, R., Kim, J., Anderson, D. J., & Guillemot, F. (2002). Divergent functions of the proneural genes Mash1 and Ngn2 in the specification of neuronal subtype identity. *Genes Dev, 16*(3), 324-338. doi: 10.1101/gad.940902

55) Petryniak, M. A., Potter, G. B., Rowitch, D. H., & Rubenstein, J. L. (2007). Dlx1 and Dlx2 control neuronal versus oligodendroglial cell fate acquisition in the developing forebrain. *Neuron, 55*(3), 417-433. doi: 10.1016/j.neuron.2007.06.036

56) Polyak, K., Lee, M. H., Erdjument-Bromage, H., Koff, A., Roberts, J. M., Tempst, P., & Massague, J. (1994). Cloning of p27Kip1, a cyclin-dependent kinase inhibitor and a potential mediator of extracellular antimitogenic signals. *Cell, 78*(1), 59-66.

57) Preisegger, K. H., Factor, V. M., Fuchsbichler, A., Stumptner, C., Denk, H., & Thorgeirsson, S. S. (1999). Atypical ductular proliferation and its inhibition by transforming growth factor beta1 in the 3,5-diethoxycarbonyl-1,4-dihydrocollidine mouse model for chronic alcoholic liver disease. *Lab Invest, 79*(2), 103-109.

58) Ross, S. E., Greenberg, M. E., & Stiles, C. D. (2003). Basic helix-loop-helix factors in cortical development. *Neuron, 39*(1), 13-25.

59) Rountree, C. B., Barsky, L., Ge, S., Zhu, J., Senadheera, S., & Crooks, G. M. (2007). A CD133-expressing murine liver oval cell population with bilineage potential. *Stem Cells, 25*(10), 2419-2429. doi: 10.1634/stemcells.2007-0176

60) Schuurmans, C., Armant, O., Nieto, M., Stenman, J. M., Britz, O., Klenin, N., . . . Guillemot, F. (2004). Sequential phases of cortical specification involve Neurogenin-dependent and -independent pathways. *EMBO J, 23*(14), 2892-2902. doi: 10.1038/sj.emboj.7600278

61) Shida, T., Furuya, M., Kishimoto, T., Nikaido, T., Tanizawa, T., Koda, K., . . . Miyazaki, M. (2008). The expression of NeuroD and mASH1 in the gastroenteropancreatic neuroendocrine tumors. *Mod Pathol, 21*(11), 1363-1370. doi: 10.1038/modpathol.2008.121

62) Shingo, T., Gregg, C., Enwere, E., Fujikawa, H., Hassam, R., Geary, C., . . . Weiss, S. (2003). Pregnancy-stimulated neurogenesis in the adult female forebrain mediated by prolactin. *Science, 299*(5603), 117-120. doi: 10.1126/science.1076647

63) Si-Tayeb, K., Lemaigre, F. P., & Duncan, S. A. (2010). Organogenesis and development of the liver. *Dev Cell, 18*(2), 175-189. doi: 10.1016/j.devcel.2010.01.011

64) Sodhi, D., Micsenyi, A., Bowen, W. C., Monga, D. K., Talavera, J. C., & Monga, S. P. (2005). Morpholino oligonucleotide-triggered beta-catenin knockdown compromises normal liver regeneration. *J Hepatol, 43*(1), 132-141. doi: 10.1016/j.jhep.2005.02.019

65) Steele-Perkins, G., Plachez, C., Butz, K. G., Yang, G., Bachurski, C. J., Kinsman, S. L., . . . Gronostajski, R. M. (2005). The transcription factor gene Nfib is essential for both lung maturation and brain development. *Mol Cell Biol, 25*(2), 685-698. doi: 10.1128/mcb.25.2.685-698.2005

66) Sugimori, M., Nagao, M., Parras, C. M., Nakatani, H., Lebel, M., Guillemot, F., & Nakafuku, M. (2008). Ascl1 is required for oligodendrocyte development in the spinal cord. *Development, 135*(7), 1271-1281. doi: 10.1242/dev.015370

67) Tan, X., Apte, U., Micsenyi, A., Kotsagrelos, E., Luo, J. H., Ranganathan, S., . . . Monga, S. P. (2005). Epidermal growth factor receptor: a novel target of the Wnt/beta-catenin pathway in liver. *Gastroenterology, 129*(1), 285-302.

68) Tan, X., Behari, J., Cieply, B., Michalopoulos, G. K., & Monga, S. P. (2006). Conditional deletion of beta-catenin reveals its role in liver growth and regeneration. *Gastroenterology, 131*(5), 1561-1572. doi: 10.1053/j.gastro.2006.08.042

69) Tomita, K., Moriyoshi, K., Nakanishi, S., Guillemot, F., & Kageyama, R. (2000). Mammalian achaete-scute and atonal homologs regulate neuronal versus glial fate determination in the central nervous system. *EMBO J, 19*(20), 5460-5472. doi: 10.1093/emboj/19.20.5460

70) Tomita, K., Nakanishi, S., Guillemot, F., & Kageyama, R. (1996). Mash1 promotes neuronal differentiation in the retina. *Genes Cells, 1*(8), 765-774.

71) Vias, M., Massie, C., East, P., Scott, H., Warren, A., Zhou, Z., . . . Mills, I. (2008). Pro-neural transcription factors as cancer markers. *BMC Medical Genomics, 1*(1), 17.

72) Vierbuchen, T., Ostermeier, A., Pang, Z. P., Kokubu, Y., Sudhof, T. C., & Wernig, M. (2010). Direct conversion of fibroblasts to functional neurons by defined factors. *Nature, 463*(7284), 1035-1041. doi: 10.1038/nature08797

73) Wakabayashi, N., Shin, S., Slocum, S. L., Agoston, E. S., Wakabayashi, J., Kwak, M. K., . . . Kensler, T. W. (2010). Regulation of notch1 signaling by nrf2: implications for tissue regeneration. *Sci Signal, 3*(130), ra52. doi: 10.1126/scisignal.2000762

74) Yun, K., Fischman, S., Johnson, J., Hrabe de Angelis, M., Weinmaster, G., & Rubenstein, J. L. (2002). Modulation of the notch signaling by Mash1 and Dlx1/2 regulates sequential specification and differentiation of progenitor cell types in the subcortical telencephalon. *Development, 129*(21), 5029-5040.

75) Zhao, L. Y., Niu, Y., Santiago, A., Liu, J., Albert, S. H., Robertson, K. D., & Liao, D. (2006). An EBF3-mediated transcriptional program that induces cell cycle arrest and apoptosis. *Cancer Res, 66*(19), 9445-9452. doi: 10.1158/0008-5472.can-06-1713

76) Zou, Y., Hu, M., Bao, Q., Chan, J. Y., & Dai, G. (2013). Nrf2 participates in regulating maternal hepatic adaptations to pregnancy. *J Cell Sci, 126*(Pt 7), 1618-1625. doi: 10.1242/jcs.118109

FIGURES

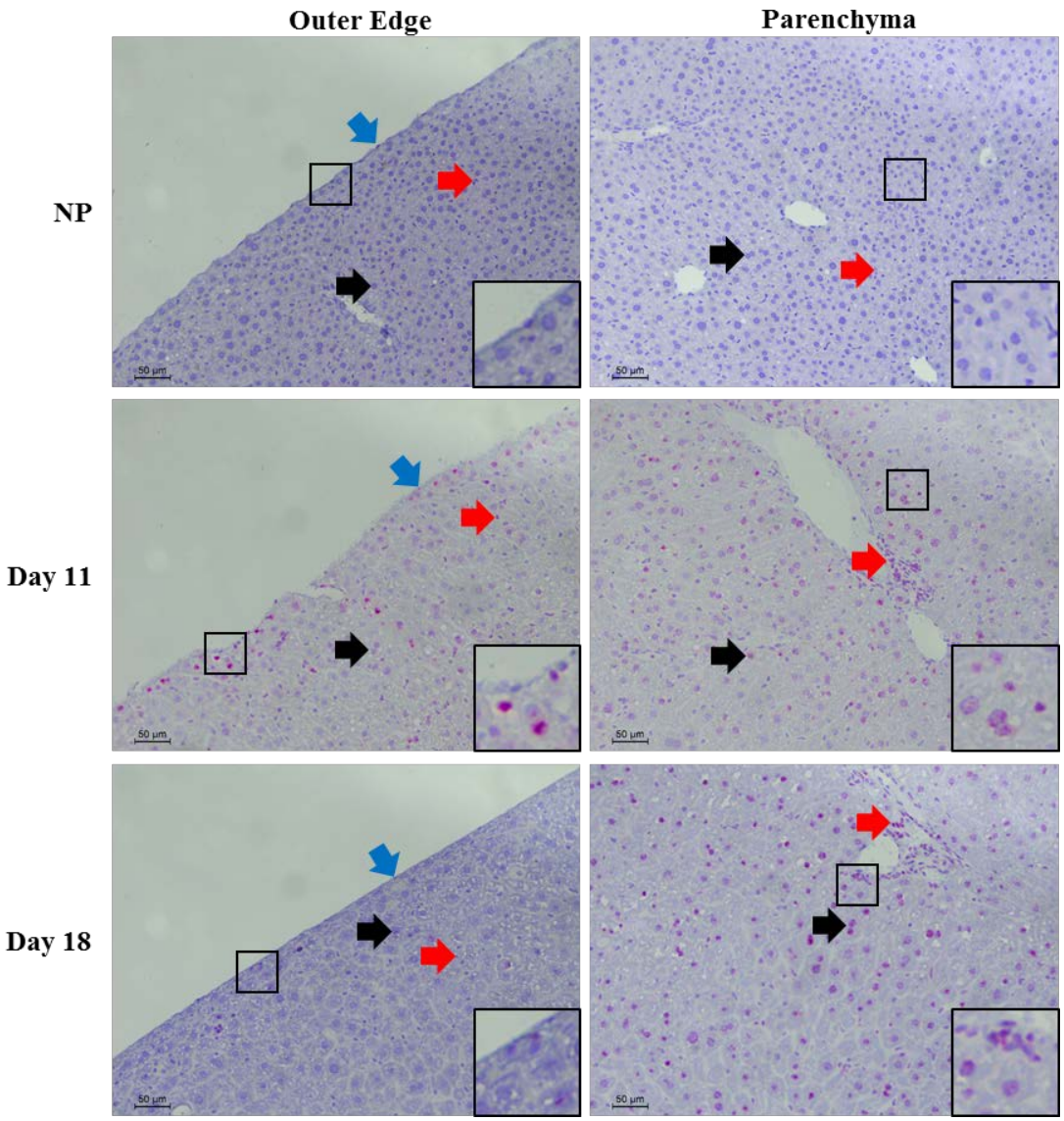

Figure 1. *In situ* hybridization for *Ascl1* mRNA in maternal liver during gestation. Nonpregnant (NP), gestation day 11 (D11), and gestation day 18 (D18) CD1 mouse livers were isolated, formalin-fixed, paraffin-embedded, and sectioned. *In situ* hybridization for *Ascl1* mRNA was performed using Fast Red from RNAscope 2.0 HD Assay, labeling the probe with red dye. Note that *Ascl1* mRNA is absent for NP liver but is present in parenchymal (black arrow), nonparenchymal (blue arrow), and mesothelial (yellow arrow) cells in pregnant liver.

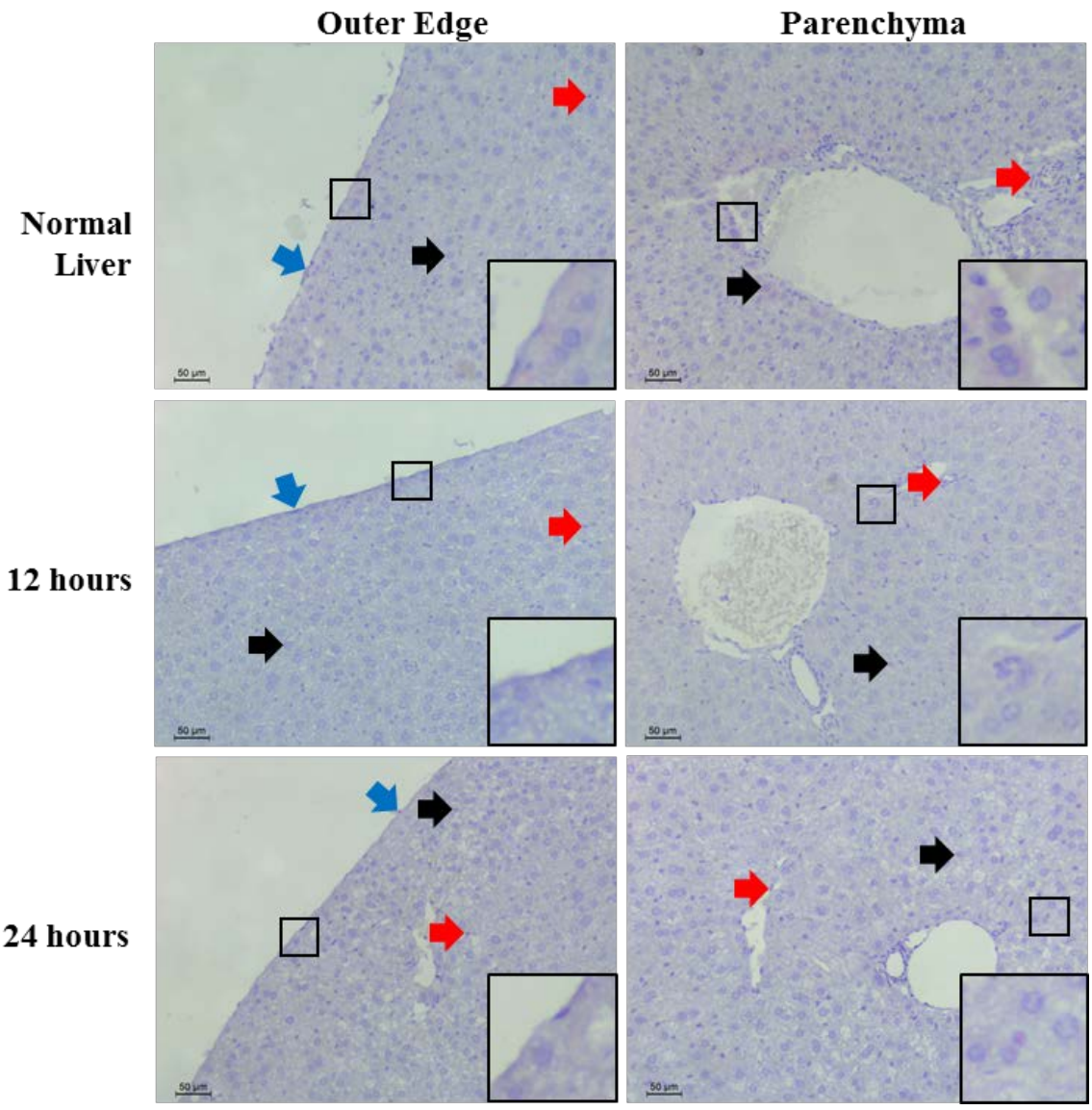

Figure 2. *In situ* hybridization for *Ascl1* mRNA in regenerating liver. Regenerating livers of 2/3 partially hepatectomized (PHx) male mice were isolated at the indicated time points after PHx, formalin-fixed, paraffin-embedded, and sectioned. *In situ* hybridization for *Ascl1* mRNA was performed using Fast Red from RNAscope 2.0 HD Assay, labeling the probe with red dye. Note that hepatic parenchymal (black arrow), nonparenchymal (blue arrow), and mesothelial (yellow arrow) cells express *Ascl1* during liver regeneration.

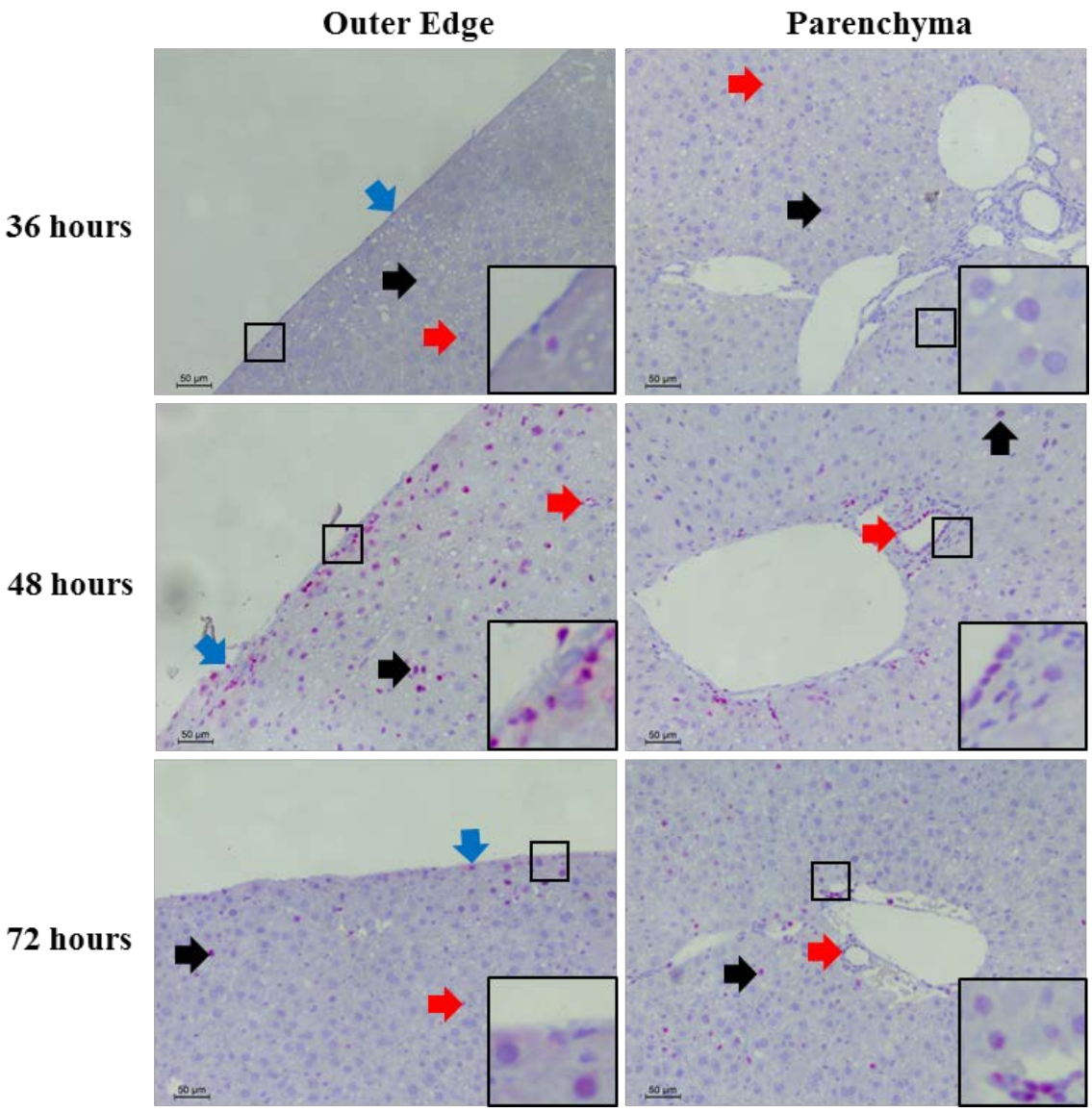

Figure 2, continued.

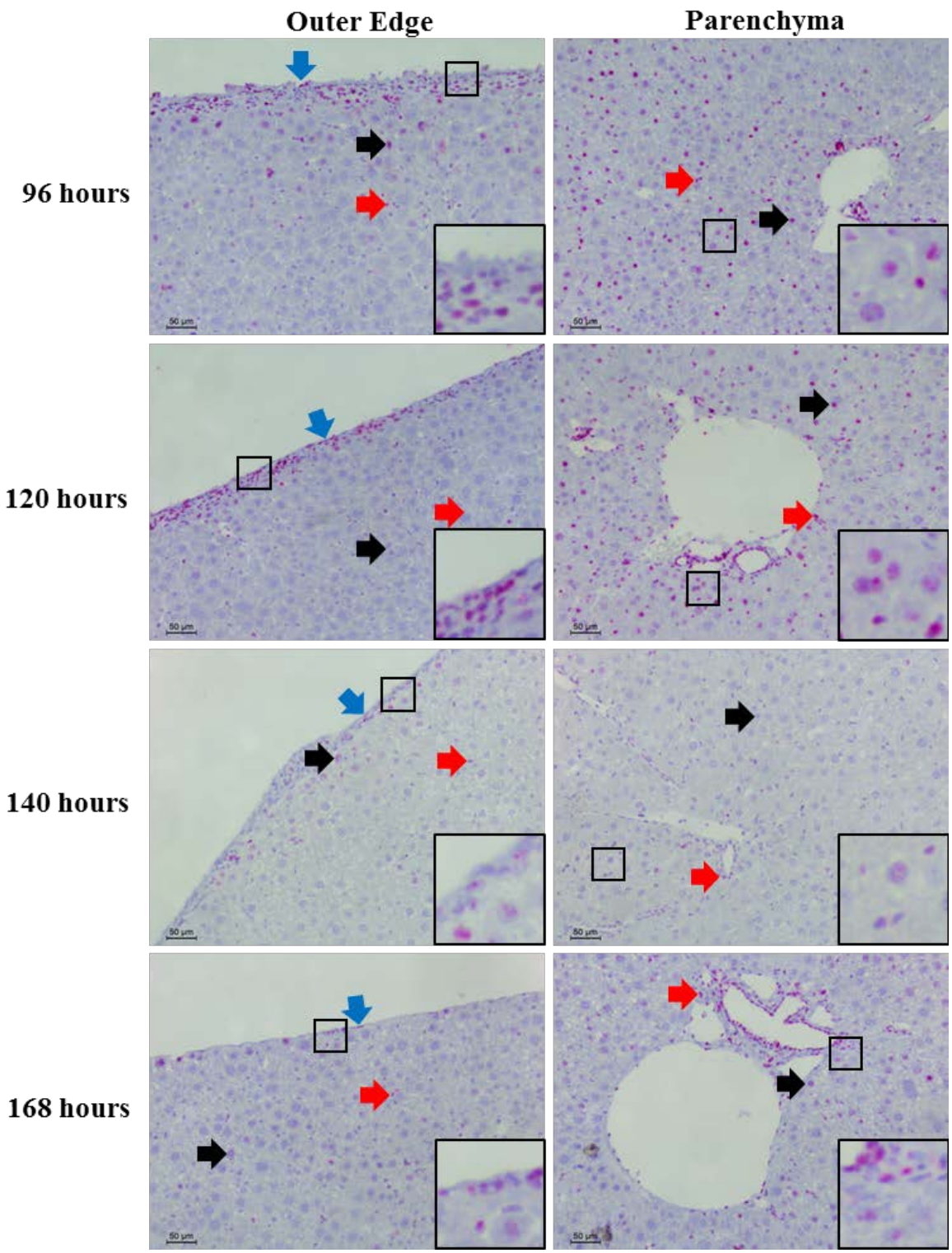

Figure 2, continued.

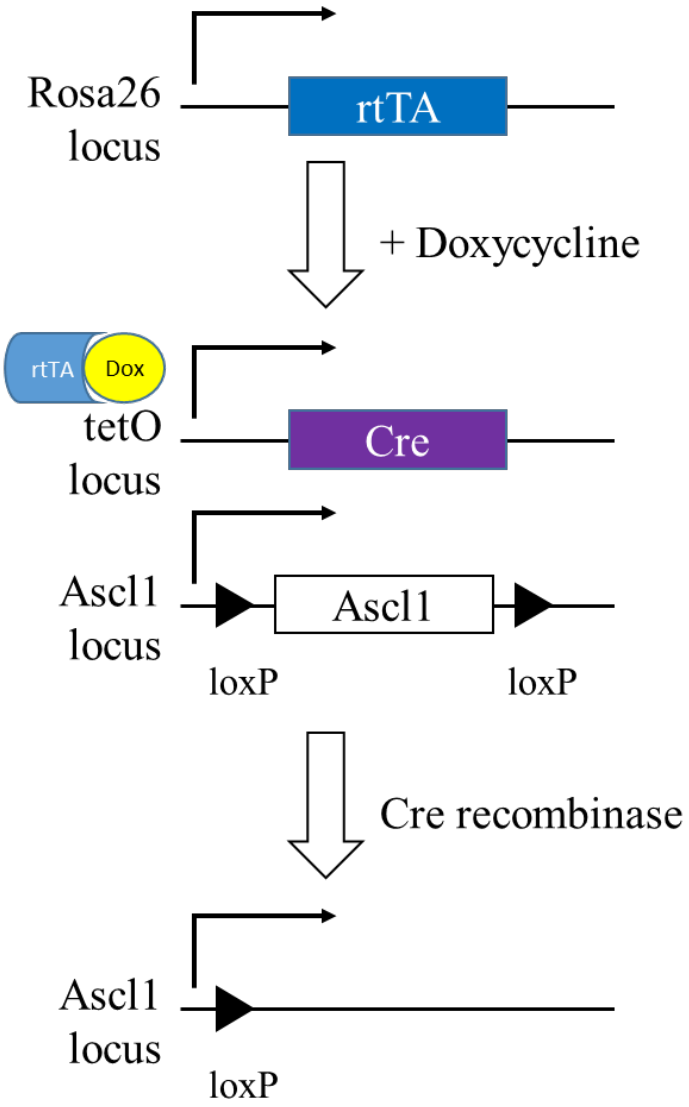

Figure 3. *Ascl1* global inducible knockout mouse model. In Ascl1$^{flox/flox}$;R26$^{rtTA/rtTA}$; tetO-cre$^{tg/-}$ mouse strain, ubiquitous Rosa26 promoter element (Rosa26 locus) drives the expression of reverse tetracycline-controlled transactivator gene (rtTA). Doxycycline (Dox) administration activates rtTA, which in turns binds to tetracycline-responsive promoter element (tetO locus) to transactivate Cre recombinase gene. Cre recombinase floxes out loxP-flanked *Ascl1* gene. As a result, *Ascl1* is ablated by doxycycline treatment.

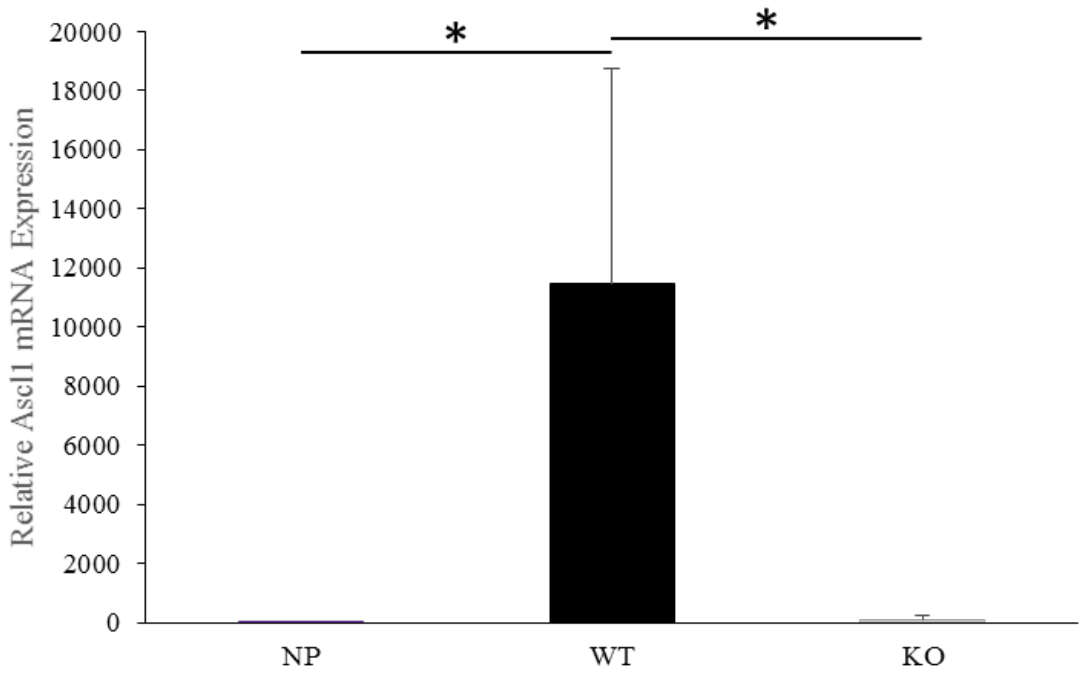

Figure 4. *Ascl1* mRNA expression in maternal liver during pregnancy. Nonpregnant (NP) and timed pregnancy was generated on genetic control (Ascl1$^{wt/wt}$;R26$^{rtTA/rtTA}$;tetO-cre$^{tg/-}$; WT) and global inducible *Ascl1* knockout (Ascl1$^{flox/flox}$;R26$^{rtTA/rtTA}$;tetO-cre$^{tg/-}$; KO) mice. Doxycycline in drinking water (1 mg/ml) was administered to pregnant mice from gestation day 6 to18. On gestation day 18, maternal livers were collected and weighed. Hepatic mRNA levels of *Ascl1* were measured by qRT-PCR and are expressed as the mean fold changes relative to NP controls (± s.d.; n=3-4. *, P<0.05).

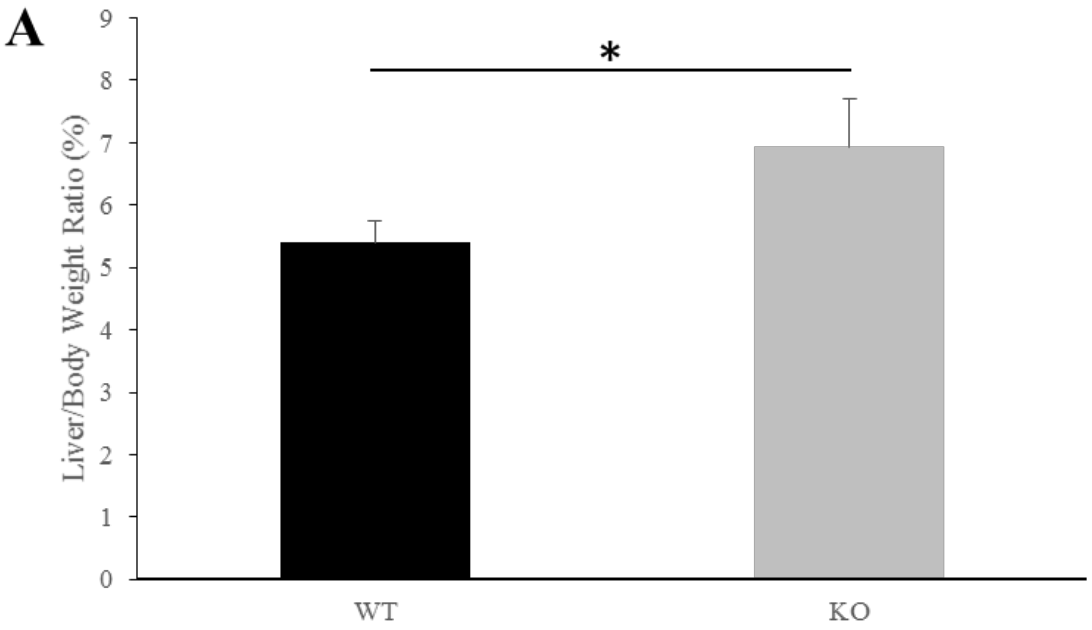

Figure 5. Phenotype from *Ascl1* ablation. Maternal livers and fetuses were collected and weighed from genetic control (WT) and KO mice (described in **Figure 4**) on gestation day 18. Maternal liver-to-body weight ratio (**A**), litter size (**B**), and fetal weight (**C**) are presented. The data are expressed as the means ± s.d.; *n*=3-4. *, *P*<0.05.

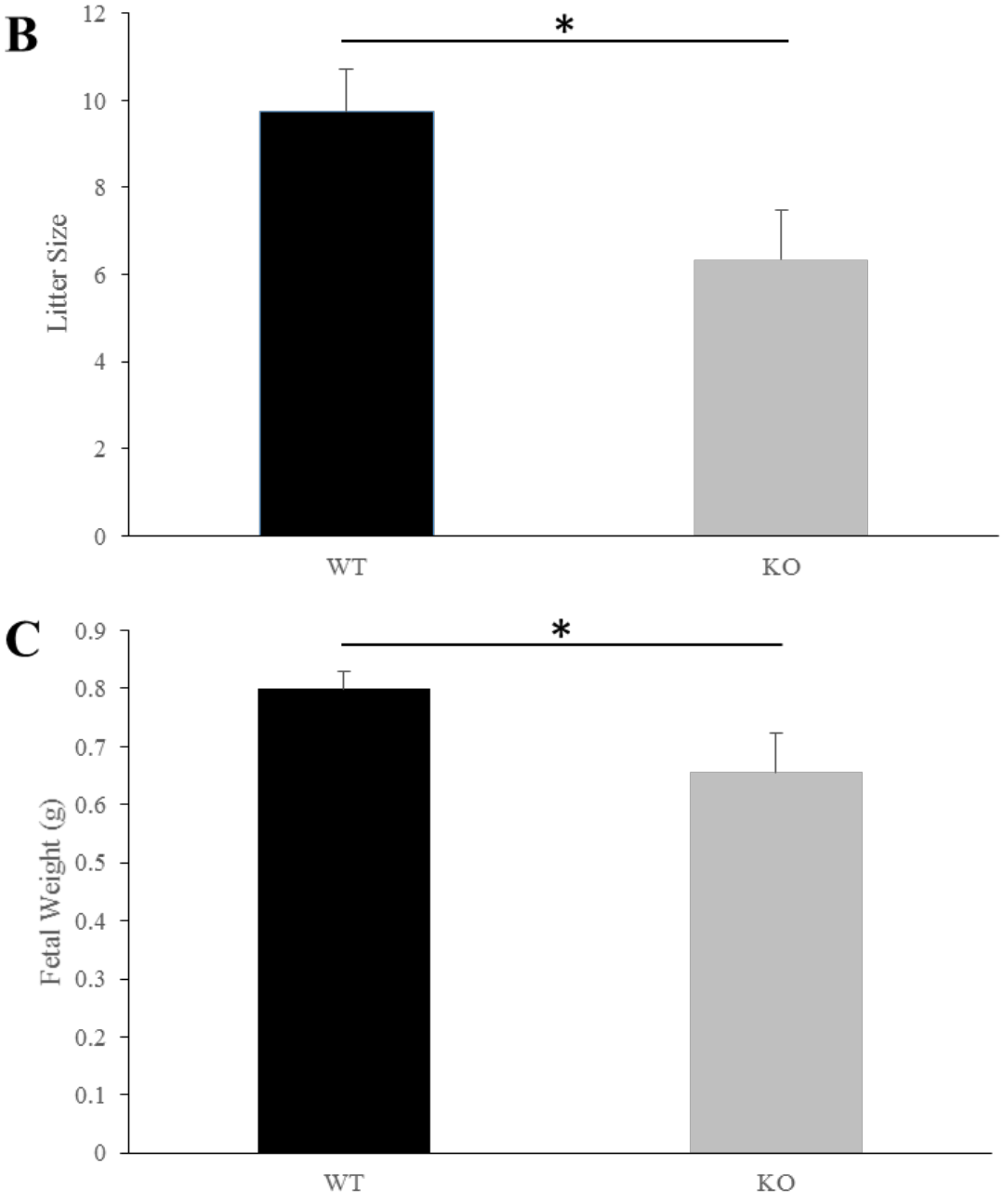

Figure 5, continued.

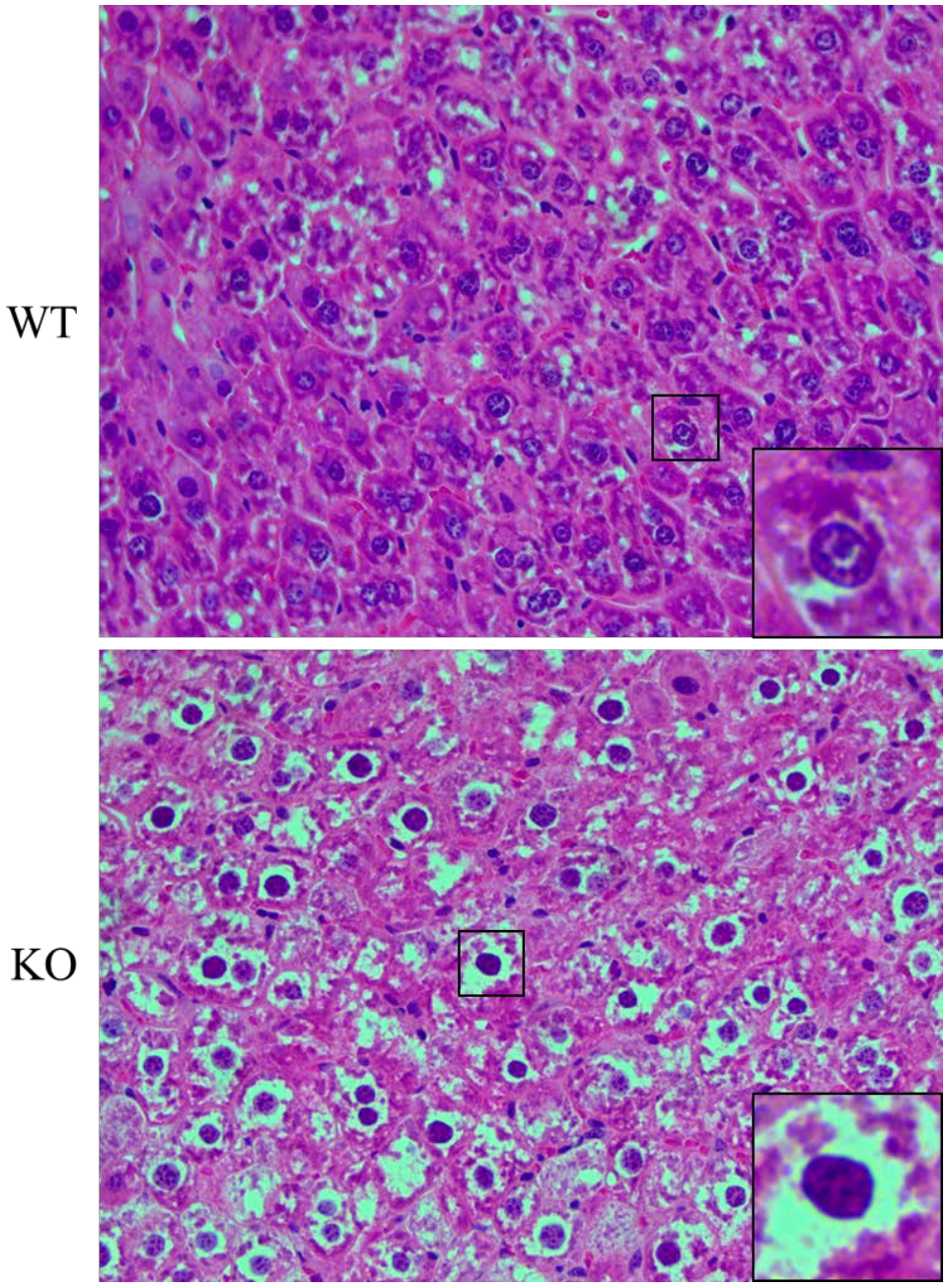

Figure 6. H&E staining of maternal liver. Maternal livers were collected from genetic control (WT) and KO mice (described in **Figure 4**) on gestation day 18, fixed in formalin, and embedded in paraffin. H&E staining was performed. Note the lack of cytosol around nuclei of hepatocytes and indistinct cellular boundaries in pregnant KO livers.

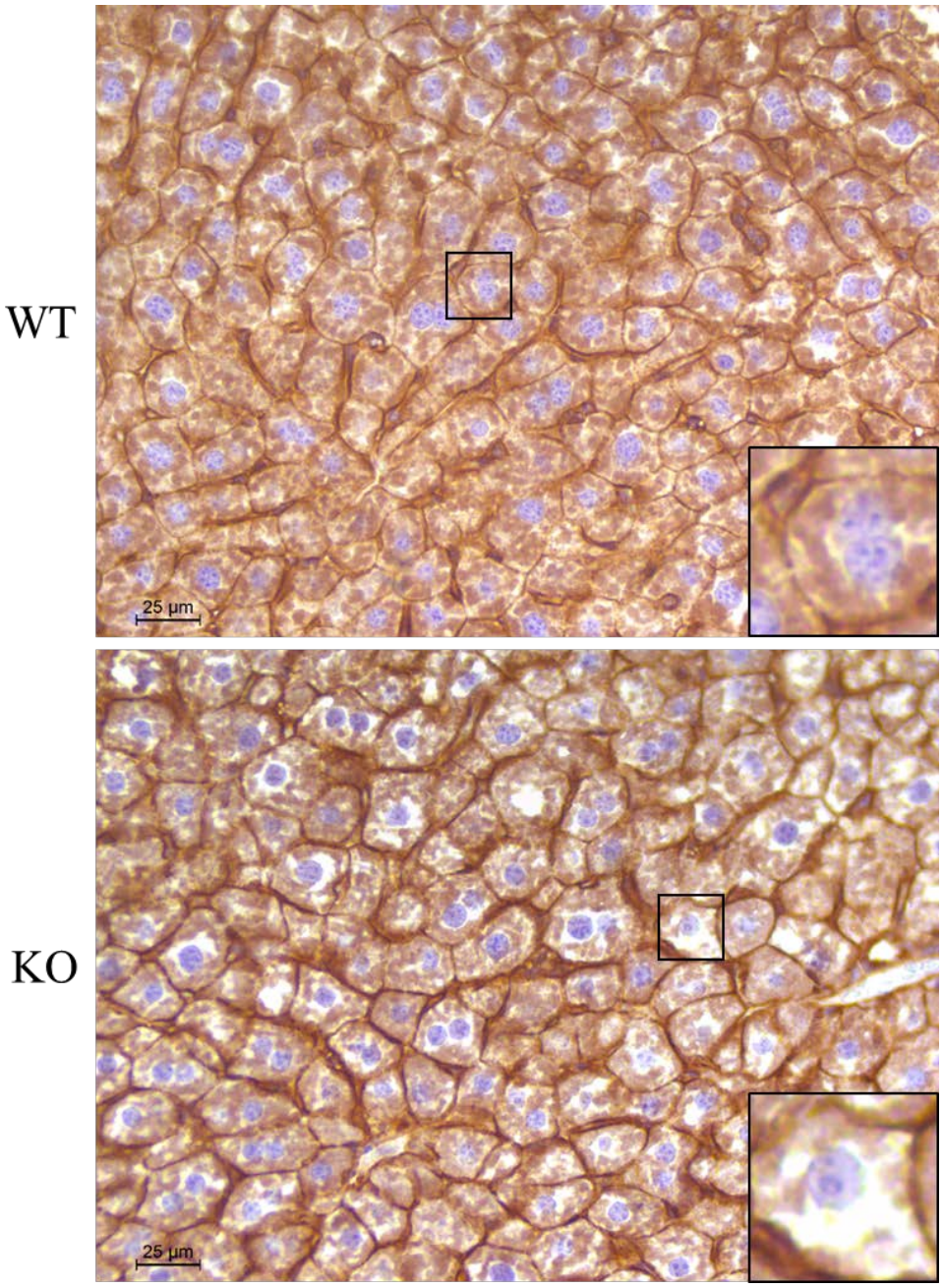

Figure 7. Pan cadherin immunostaining. Maternal livers were collected from genetic control (WT) and KO mice (described in **Figure 4**) on gestation day 18, fixed in formalin, and embedded in paraffin. Pan cadherin immunostaining was performed. No overt differences in cell-cell junction between WT and KO maternal livers were observed.

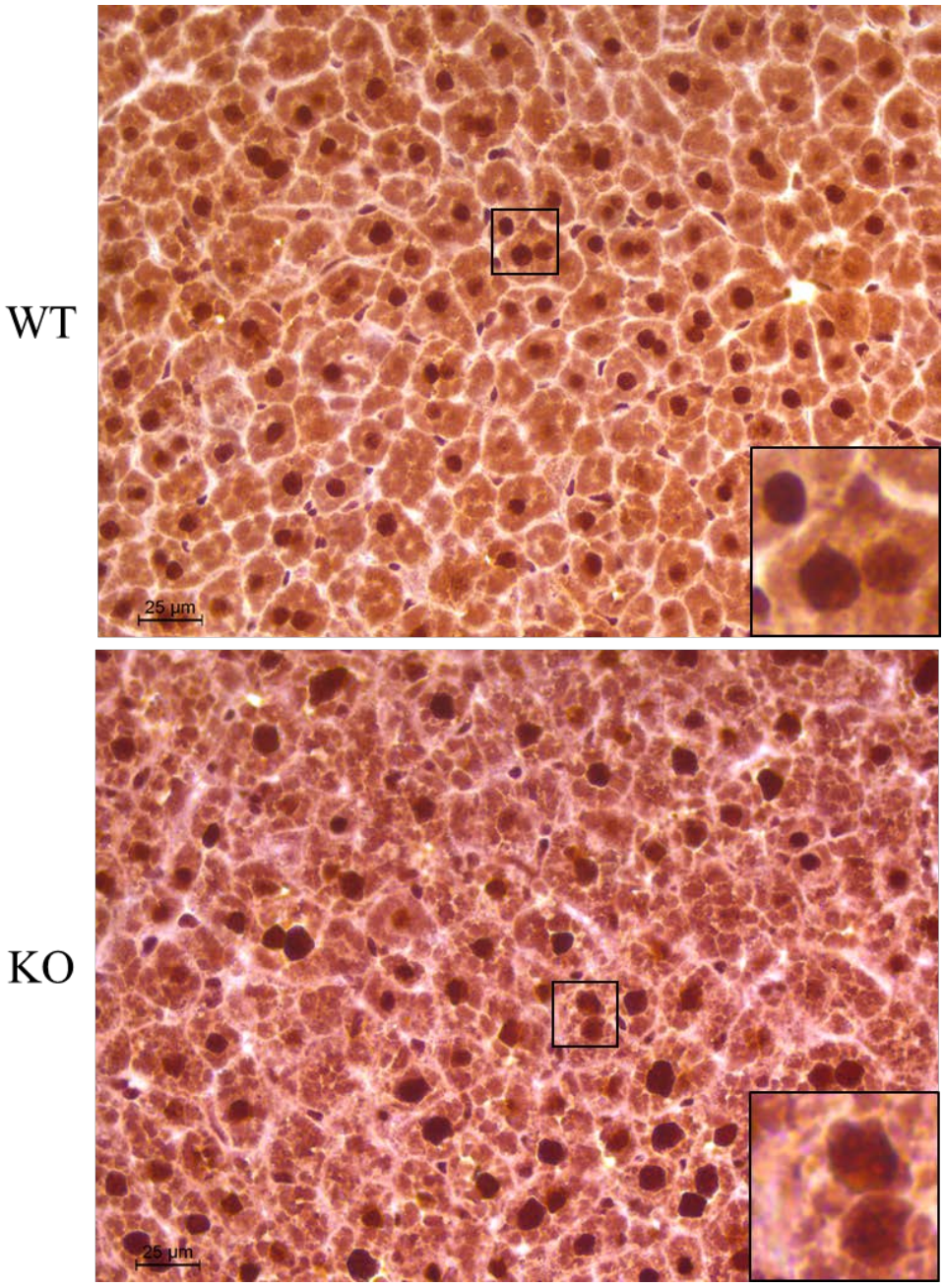

Figure 8. Hepatocyte nuclear factor 4 alpha (HNF4α) immunostaining. Maternal livers were collected from genetic control (WT) and KO mice (described in **Figure 4**) on gestation day 18, fixed in formalin, and embedded in paraffin. HNF4α immunostaining was performed. HNF4α was positive in nuclei of hepatocytes in both WT and KO maternal livers.

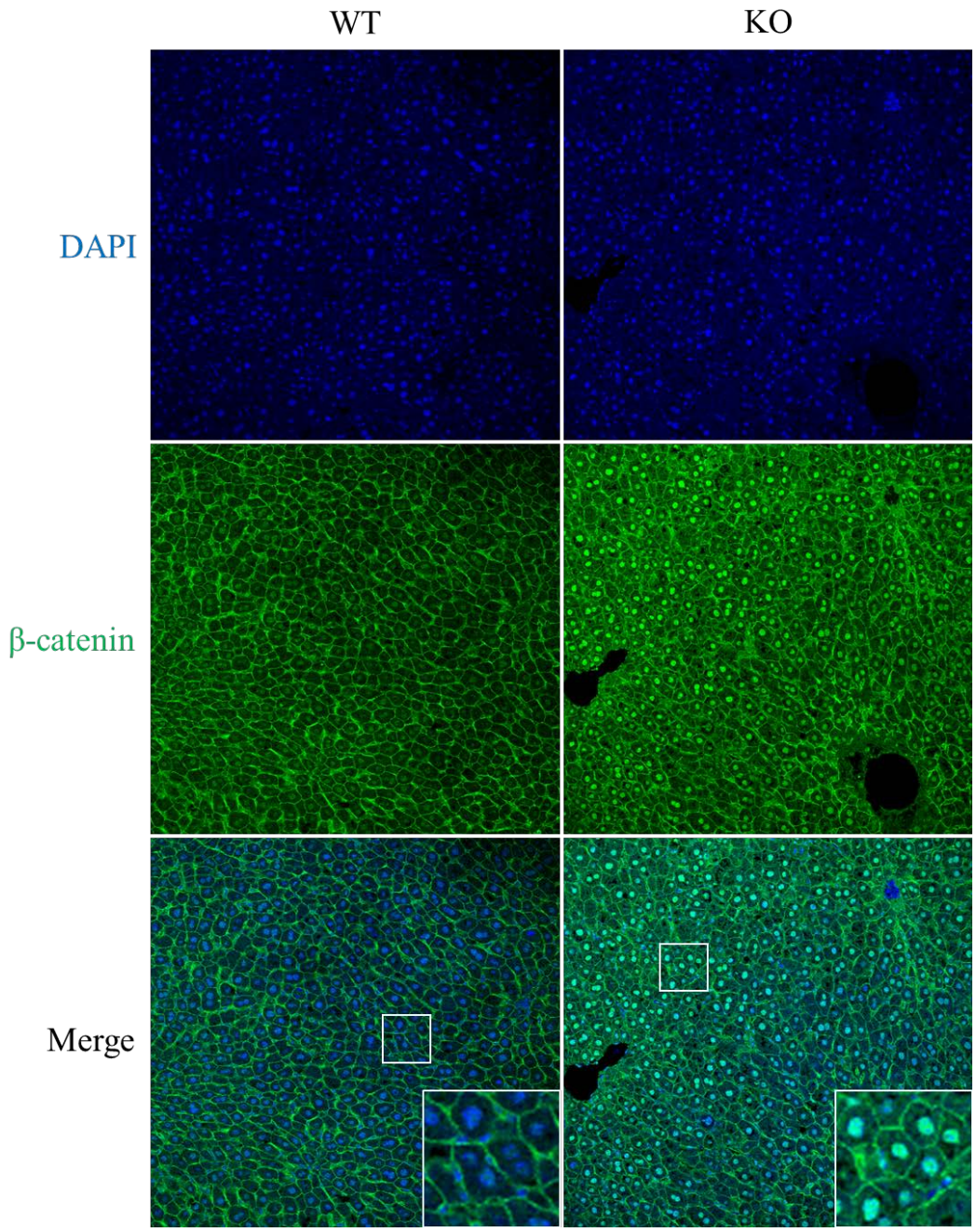

Figure 9. β-catenin immunofluorescence staining. Maternal livers were collected from genetic control (WT) and KO mice (described in **Figure 4**) on gestation day 18, fixed in formalin, and embedded in paraffin. β-catenin immunofluorescence staining was performed. Note the increased nuclei translocation of β-catenin in KO livers compared to controls (400x magnification).

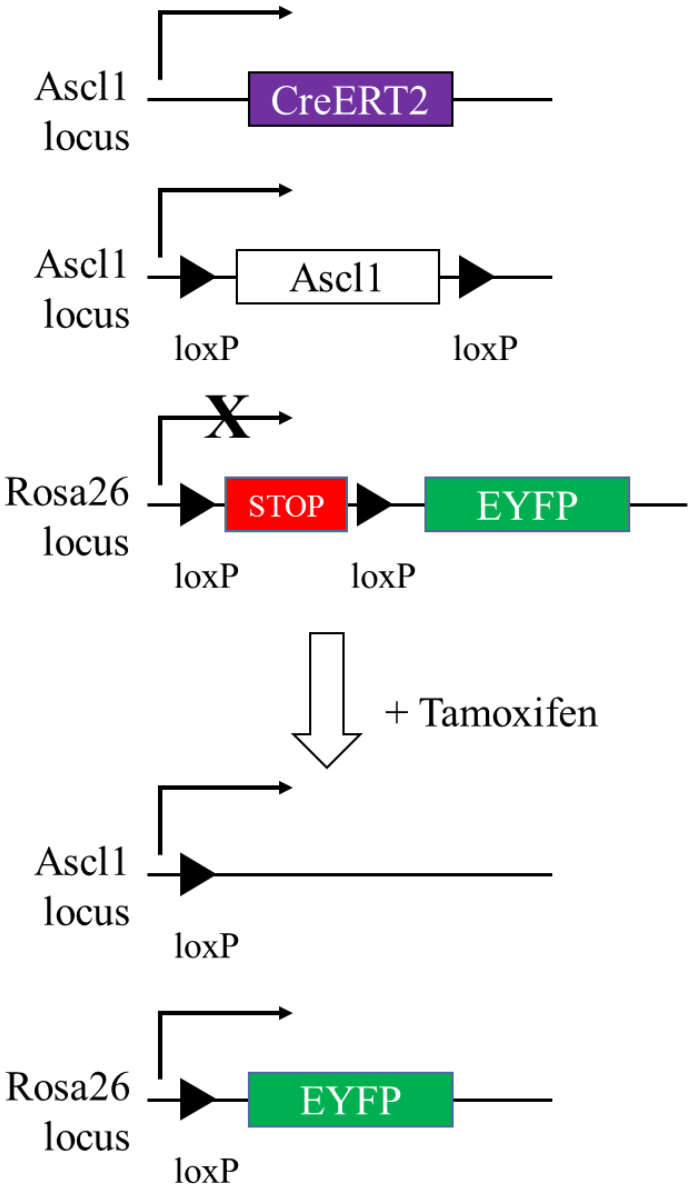

Figure 10. *Ascl1* cell-specific conditional and inducible knockout mouse model. In Ascl1$^{flox/CreERT2}$;R26$^{stopfloxYFP/stopfloxYFP}$ mouse strain, *Ascl1* promoter element (Ascl1 locus) drives the expression of Cre recombinase gene. Tamoxifen administration activates Cre recombinase, which in turns floxes out loxP-flanked *Ascl1* gene and loxP-flanked STOP sequence. As a result, *Ascl1* is specifically ablated in *Ascl1*-expressing cells by tamoxifen treatment.